LASER INTERFEROMETER GRAVITATIONAL WAVE OBSERVATORY
– LIGO –
CALIFORNIA INSTITUTE OF TECHNOLOGY
MASSACHUSSETS INSTITUTE OF TECHNOLOGY

Document Type **LIGO T990077-00-D** 17 Aug 99
Low Thermal Noise Accelerometers for the Active Control of a Very Low Frequency Seismic Isolator
A. Bertolini, R. DeSalvo, F. Fidecaro, M. Francesconi

Distribution of this draft:
LIGO Detector and LIGO Systems Engineering

This is an internal working note
of the LIGO Project.

California Institute of Technology
LIGO Project -MS 51-33
Pasadena, CA 91125
Phone (626) 395-2129
Fax (626) 304-9834
E-mail: info@ligo.caltech.edu

Massachussets Institute of Technology
LIGO Project - MS 20B-145
Cambridge, MA 01239
Phone (617) 253-4824
Fax (617) 253-7014
E-mail: info@ligo.mit.edu

WWW: http://www.ligo.caltech.edu/

1. Introduction

To achieve the required seismic isolation of the interferometer mirrors in all the six degrees of freedom (DOF), we propose the use of a chain made of a mix of active and passive techniques based on the inverted pendulum (IP) and GAS standard filter geometries. A crucial point is to keep the RMS residual motion on the bottom of the chain within the dynamic range of the mirrors actuators, to allow the interferometer to be stably locked and to reduce the dynamic range requirements on the actuators themselves. In a purely passive seismic isolator the payload is essentially driven by the low frequency mechanical resonances of the first stages of the attenuation chain; therefore in order to reduce the RMS mirrors displacement it is fundamental to drain the stored energy from these resonances (inertial damping), obviously avoiding to degrade the chain quality factor and to inject in the frequency range of interest undesirable noise from sensors and actuators. It is also desirable to actively reduce the amount of seismic activity in the frequency region of the mechanical resonances (active seismic attenuation). The VIRGO collaboration clearly showed [1] the benefits, for this task, of the active inertial damping freezing the RMS payload motion from few tens of microns to few hundreds of nanometers, by putting on the top of the isolation chain a feedback actuated platform with a very low resonant frequency (30 mHz). The SAS chains will also operate with a VIRGO-like active damped preisolating platform but, in order to further reduce the RMS noise and to keep it within few nanometers, a nested second level of feedback control, based on high performance accelerometers, may be implemented on the system (Fig.1).

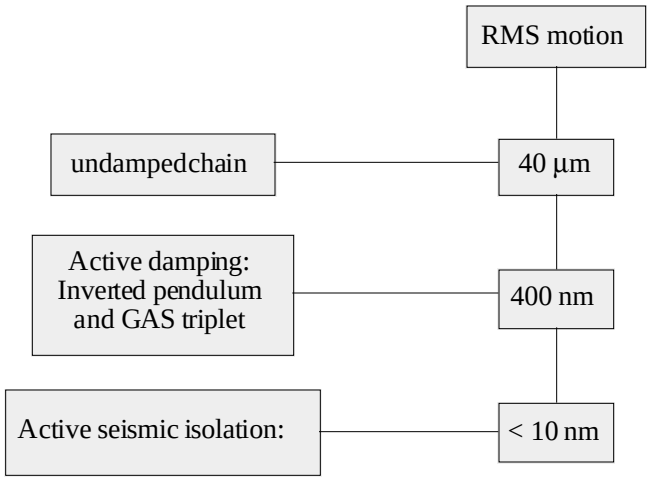

Fig. 1 Active control strategy

A sufficient level of pre–attenuation before the high performance accelerometers is necessary because the accelerometers themselves are partially sensitive to accelerations orthogonal to their axis of sensitivity. If the seismic activity in the orthogonal direction is not pre–attenuated, using the aacelerometer in feedback loop would result in the injection of the orthogonal perturbation on the direction of interest. In this case the amount of the injected noise is equal to the accelerometer sensitivity to the transversal axis. In designing the accelerometer it will then be important to use configurations in which the test mass is free on the desired axis but is rigidly constrained in all other directions. The residual transversal axis sensitivity must be treated by nesting attenuation stages. In principle this problem could be treated by 6 DOF MIMO's but this approach proved to be hard and unreliable and it was abandoned by VIRGO in favour of 3 DOF mechanical systems and MIMOs.

This task places strong requirements on the sensitivity of the accelerometers to be used, in order to avoid the re–injection of undesired noise fron the feedback system itself. A reasonable constraint is the signal–to–noise ratio of the control system to be at least between 10 and 100 in the frequency region around the resonance to be damped, typically from 0.01 to 2 Hz. In this case the signal level is defined as the target seismic noise level. For example, while in the first level of active isolation the sensitivity required from the accelerometers to damp a resonant frequency of 30 mHz is about $10^{-9}\,\mathrm{m}/\sqrt{\mathrm{Hz}}$, in the second one the minimum useful requirement becomes $10^{-11}\,\mathrm{m}/\sqrt{\mathrm{Hz}}$. Accelerometers of design directly derived from the VIRGO ones [2] have enough sensitivity to

satisfy the constraint for the preisolator active damping, but, as it will be shown, they are inadequate to reach the target RMS residual noise, essentially because of the mechanical losses which dominates the device performance at low enough frequencies. In this document we present concepts and features of a new horizontal accelerometer whose mechanical design and machining process aim to improve the sensitivity at very low frequencies; the potential performances are also evaluated. The use of these accelerometers will allow a true active seismic pre–attenuation in front of the passive chain and it will further extend the possibility of using low noise injection drives instead of the electromagnetic or electrostatic drives to control the mirrors. The design concepts of this horizontal accelerometer could be valid to be applied to the design of a vertical accelerometer and of a high sensitive tiltmeter.

2. The state of art and our design concepts

An accelerometer essentially consists in a mass oscillating along one degree of freedom and a displacement sensor which monitors the mass position with respect to its suspension point. The sensor output is filtered and fed back to the mass through a force transducer which holds the mass on its equilibrium position; the voltage driving the force transducer is directly proportional to the acceleration of the support of the device within the control bandwidth. The feedback operation is a fundamental issue allowing to use a mechanics with an high Q factor without saturation of the device response, and to clean the accelerometer output signal from spurious mechanical resonances.

The parameters relevant to evaluate the quality of an accelerometer are the directionality, that is the insensitivity of the device to accelerations orthogonal to that of measurement, the position sensor noise and, at very low frequencies (below 1 Hz), the thermal noise associated with the friction processes in the mechanics. Additionally, for our use, the accelerometers must be fully UHV compatible and have low power consumption. At present the best performant low frequency device are the accelerometers developed by VIRGO group to be used in the active damping of the chain preisolating platform [1]. The position sensor is a Linear Variable Differential Transformer (LVDT) which is composed (Fig. 2) by a primary winding, fed with a 50 kHz modulation signal, and by a secondary winding composed by two coils, symmetric with respect to the primary one and wound in opposite directions.

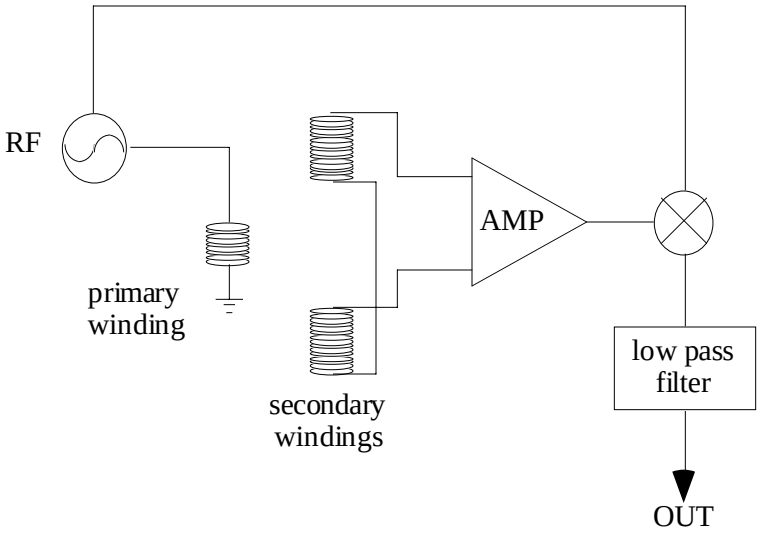

Fig. 2 Schematic of an LVDT displacement sensor; the primary winding has been moved sideways for simplicity.

The three coils are mounted coaxially to be in close electromagnetic contact like in a transformer. The primary coil is mounted on the test mass and the secondaries on the device's frame. The mixer output is a DC signal proportional to the relative displacement between the two LVDT windings. A schematic drawing of a VIRGO–like accelerometer is shown below:

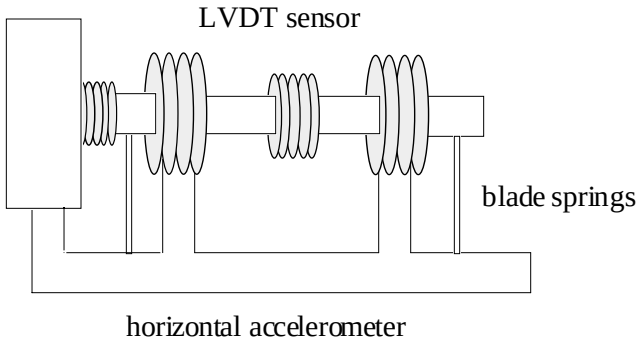

Fig.3 Schematic drawing of an horizontal accelerometer based on an inverted pendulum

The test mass is mounted on a small inverted pendulum sustained by two Cu–Be blade springs; the mass is 0.5 Kg and the resonant frequency is about 0.5 Hz. The accelerometer operates in closed loop: the LVDT senses the displacement and a voice–coil actuator, also mounted coaxially to the three coils on the accelerometer sensitive axis can push or pull on the test mass to keep the LVDT output null. While the sensitivity of the LVDT is very good, about $10^{-11}\mathrm{m}/\sqrt{\mathrm{Hz}}$, the clamp

friction of the blade springs degrades the device performances at frequencies below 1 Hz. The displacement spectral sensitivity of an accelerometer due to the thermal noise is given by [3]:

$$\tilde{x}_{th.noise} = \sqrt{\frac{4K_B T \omega_0^2}{MQ\omega^5}} \qquad (2.1)$$

where M, ω_0 and Q are respectively the mass, the resonant frequency and the quality factor of the accelerometer. The previous equation is valid supposing an internal friction damping mechanism; typically the Q factor for these devices is only between 10 and 30 resulting in a noise level of the order of 10^{-9}m/$\sqrt{}$Hz around 100 mHz. For these characteristics the device is suitable for the first level of the active control but it is inadequate for the second one. According to equation (1) one can increase the accelerometer performances by decreasing its resonant frequency, increasing its mass and increasing the Q factor; starting from these constraints the folded pendulum [4] geometry can be very helpful to design a horizontal accelerometer, allowing very low resonant frequencies (also below 100 mHz) and an high Q factor.

2.1 The folded pendulum

The folded pendulum has been introduced by ACIGA group both to build an ultra–low frequency pre–isolation stage for a laser interferometer gravitational wave detector and as an acceleromter mechanics. A folded pendulum (FP) is essentially a mass suspended on one side by a simple pendulum and on the other by an inverted pendulum working antagonistically. In this way the straight pendulum positive gravitational spring constant is balanced by the inverted pendulum negative gravitational spring constant; the only dissipation is in the mechanics elastic flexures and in the readout/actuation system. If the elastic flexure spring constant is minimized, the mechanical losses are minimal and large Q–factors are possible; by carefully shaping the mass it is also possible to lower arbitrarily the resonant frequency until the system collapses. As shown in Fig.3 the inverted pendulum arm has a hook shape to allow all the pivot flexures to work in tension in order to have small elastic restoring forces and still avoid buckling problems.

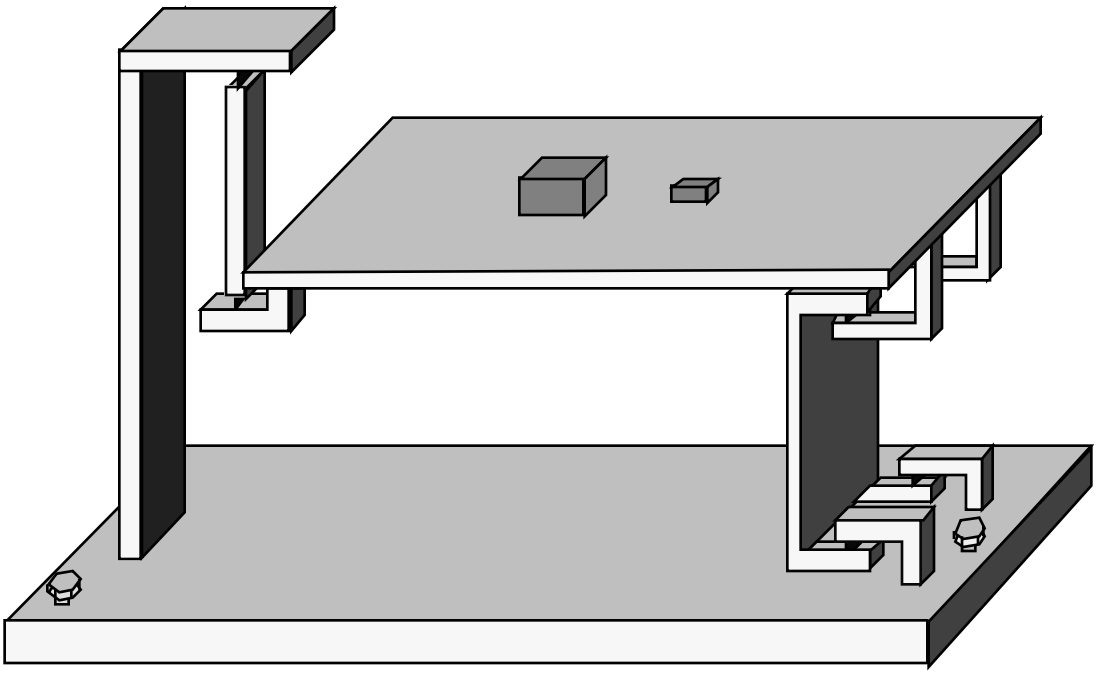

Fig.4 The folded pendulum prototype built by the ACIGA group.

The simplest model of an FP consists in a simple pendulum with equivalent mass M_{e1} and length L_{e1} and an inverted pendulum with equivalent mass M_{e2} and length L_{e2} connected by a massless rigid beam.

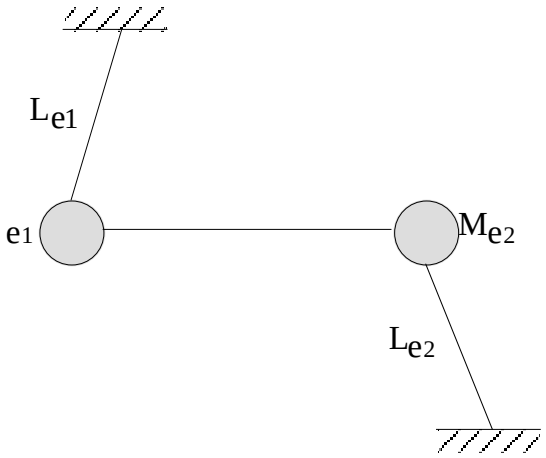

Fig.5 Simple model of a folded pendulum

The equivalent masses and lengths take into account of the momentum of inertia of the rigid arms. In small angle approximation the gravitational restoring force of the system is:

$$F = -\left(\frac{M_{e1}g}{L_{e1}} - \frac{M_{e2}g}{L_{e2}}\right)x \qquad (2.1.1)$$

and the resonant frequency is:

$$\omega_0 = \sqrt{\frac{g}{(M_{e1}+M_{e2})}\left(\frac{M_{e1}}{L_{e1}} - \frac{M_{e2}}{L_{e2}}\right) + \gamma} \qquad (2.1.2)$$

where γ takes into account of the stiffness of the supporting flex joints. Depending ω_0 essentially only on the position of the center of mass of the system, an arbitrarily low resonant frequency can be obtained; actually when

$$\left(\frac{M_{e1}}{L_{e1}} - \frac{M_{e2}}{L_{e2}}\right) < 0 \qquad (2.1.3)$$

the system becomes unstable and it collapses. A more detailed model is necessary for the FP design and to evaluate accurately the mechanical frequency response. Consider two vertical arm having the same length L and different masses m_{a1} and m_{a2} ; in this model the oscillating load M is represented, depending on its center of mass position with respect to the two pendula, through two equivalent masses m_{p1} and m_{p2}.

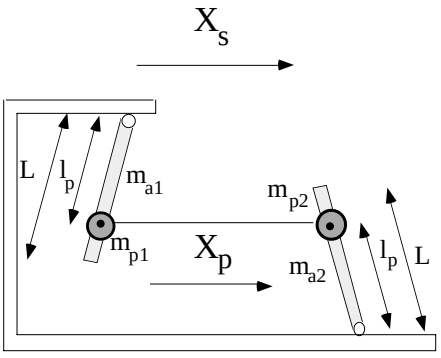

Fig.6 Model of a FP taking into account the momentum of inertia of the arms

In Fig.5 X_s and X_p are respectively the coordinates of the frame and of the pendulum center of mass, while l_p is the distance between the pivot point of the pendulum arm and the hinging point of

the oscillating mass; for a good thermal stability is useful the pendulum length l_p to be equal for both of the arms because, with an asymmetry, a temperature change can produce a tilt of the oscillating mass, then a drift of the equilibrium position.
By solving the Lagrange equations of the system of Fig.5 in the frequency domain [4] the frequency response is:

$$\frac{X_p}{X_s} = \frac{1 - A\dfrac{\omega^2}{\omega_0^2}}{1 - \dfrac{\omega^2}{\omega_0^2}} \tag{2.1.4}$$

where the parameter A and ω_0, considering beams as pendulum arms, are given by:

$$A = \frac{\left(\dfrac{L}{3\,l_p} - \dfrac{1}{2}\right)\left(m_{a1} + m_{a2}\right)}{\dfrac{L}{3\,l_p}\left(m_{a1} + m_{a2}\right) + \left(m_{p1} + m_{p2}\right)\dfrac{l_p}{L}} \tag{2.1.5}$$

$$\omega_0^2 = \frac{\dfrac{1}{2}\left(m_{a1} - m_{a2}\right)\dfrac{L}{l_p} + \left(m_{p1} - m_{p2}\right)}{\dfrac{1}{3}\left(m_{a1} + m_{a2}\right)\dfrac{L^2}{l_p^2} + \left(m_{p1} + m_{p2}\right)} \cdot \frac{g}{l_p} \tag{2.1.6}$$

We can also compute the equivalent mass M_e of the system:

$$M_e = \frac{1}{3}\left(m_{a1} + m_{a2}\right)\frac{L^2}{l_p^2} + \left(m_{p1} + m_{p2}\right) \tag{2.1.7}$$

The factor A originates from the fact that the two arms of the FP are made of rigid bars, so that the positions of the hinges with respect to the arms affect the transfer function of the pendulum, as shown in Fig.7.

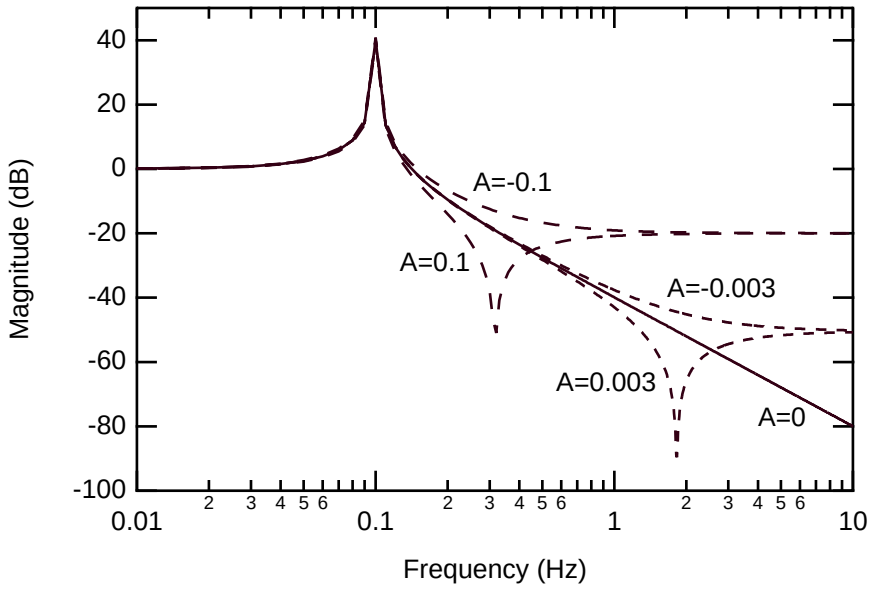

Fig.7 Calculated transfer function of an FP for different values of the parameter A

A solution to reduce this effect is to locate one of the flexures exactly on the center of percussion of each arm. Furthermore unlike in the use of the folded pendulum as vibration isolator, in the application of the FP as an accelerometer this effect is much less critical due to feedback loop operation.

Taking into account also the contribution of the flex joints the resonant frequency is given by:

$$\omega_0^2 = \frac{\kappa_{grav} + \kappa_{flex}}{M_e l_p^2} = \frac{g l_p \Delta M + \kappa_{flex}}{M_e l_p^2} \qquad (2.1.8)$$

where the ΔM is:

$$\Delta M = \frac{1}{2}(m_{a1} - m_{a2})\frac{L}{l_p} + (m_{p1} - m_{p2}) \qquad (2.1.9)$$

According to Blair et al.[5], if the load M is supported by n identical flexures in tension, the corresponding spring angular stiffness κ_{flex} is:

$$\kappa_{flex} = \sqrt{2n\, E\, I\, Mg} \qquad (2.1.10)$$

where E is the Young modulus of the material and I is the momentum of inertia of the cross section of the flexure. I for a rectangular flex joint of thickness d and lateral dimension a is:

$$I = \frac{a\, d^3}{12} \qquad (2.1.11)$$

Thus the flexure stiffness can be strongly reduced by decreasing the joint thickness being the only limitation the yield strength of the material. Typical κ_{flex} is a couple of order of magnitude smaller than the gravitational term κ_{grav},which determines the resonant frequency of the FP. As it will be shown in next section the flexure spring stiffness controls the dissipative behaviour of a folded pendulum when the other sources of damping like the gas and clamp friction are eliminated.

2.2 The Q factor of a folded pendulum

In order to enhance the low–frequency performances of the accelerometer is fundamental to increase the Q factor of the mechanical oscillator. The accelerometer will work under high vacuum; hence, having excluded the gas damping, the only dissipative effects are the structural ones. The structural damping arises substantially from two effects: the first one is the so called "stick–and–slip" mechanism arising from boundary shear effects between surfaces of distinguishable mechanical parts in contact; if present it is often the dominating and most insidious effect. The second one is the "internal" damping associated with the internal friction in a volume of solid material. In a folded pendulum the damping forces are localized in the internal friction of flexures which allow the movement of the test mass and in the clamp friction at the junctions between flexures and clamps (Fig.8), characteristic for this kind of suspension [6].

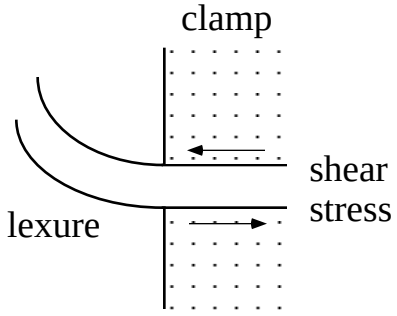

Fig.8 Picture of the clamp friction effect

As demonstrated by Cagnoli et al.[7] this effect can be reduced by localizing the clamping pressure in a small surface or eliminated altogether the clamps by means of shaped monolithic joints. The internal friction can be represented [3] by modifying the Hooke law introducing a complex elastic constant K:

$$K = K_e(1 + i\varphi) \qquad (2.2.1)$$

where φ, the loss angle, is defined as the reciprocal of the Q factor. We can assume Q to be frequency independent [3]. The term K_e is simply defined as:

$$K_e = \frac{\kappa_{grav} + \kappa_{flex}}{l_p^2} \qquad (2.2.2)$$

The loss angle is equal to the fraction of the mechanical energy stored in the pendulum flexures which is lost in each cycle of oscillation; as previously shown most of the energy stored in a folded pendulum is gravitational and only the elastic energy stored in the flexures can be dissipated. Thus there is a beneficial dilution effect of the Q factor and the effective loss angle of the FP can be less than the intrinsic one of the material

$$\varphi_{eff} \approx \varphi_{mat} \frac{\kappa_{flex}}{\kappa_{grav}} = \varphi_{mat} \cdot \frac{\sqrt{2n\ E\ I\ Mg}}{g\ l_p\ \Delta M} \qquad (2.2.3)$$

By using high strength, low loss materials like Cu–Be, maraging steel or glassy alloys one can design very thin flexures (10–20 μm) to support masses of few kilos; being I proportional to the cube of the joint thickness one can easily obtain a dilution factor from 2 to 50 with a resonant frequency of 200 mHz, also in a small folded pendulum with arm length less than 10 cm.

3. The horizontal accelerometer

3.1 Mechanics and machining techniques

Starting from the concepts expressed in the last paragraph we are building a prototype of an

horizontal accelerometer based on the folded pendulum geometry. In order to keep as low as possible the thermal noise we eliminated all the clamps from the mechanics of the accelerometer; we obtain the test mass, the joints and the external structure by EDM (electrical discharge machining) machining the mechanics from a single piece of material. Wire EDM is a method to cut conductive materials with a thin electrode that follows a computer controlled path. The electrode is a thin wire with a diameter ranging from 50 to 300 μm; the accuracy of machining is of the order of 5 μm. The hardness of work material has no detrimental effect on the cutting precision because there is no physical contact between the wire and the part being machined. The wire, immersed in de–ionized water, is charged at high voltage until a spark jumps the gap and erodes a small portion of the work piece. The de–ionized water cools and flushes away the removed particles from the gap. Each individual spark generates a small crater in the material to be cut; consequently EDM surfaces is not sufficiently accurate to machine directly the flex joints with a thickness between 10 and 30 μm; for this reason the flexures will be only pre–shaped by EDM and they will be finished through a more accurate process, the electropolishing.

In electropolishing the material is electrochemically removed ion by ion from the surface of the metal object being polished; this technique allows to remove thin layer of material (few microns) with a high degree of accuracy. Basically the process is the reverse of the electroplating: the work piece is immersed in an electrolyte and subjected to a DC electrical current, the work piece being the anode and a nearby metal electrode the cathode; the material is removed as metallic salt. The polishing effect is electric field driven; due to this fact the microasperities of the surface make the electrical field higher and the material removal is more effective. The EDM craters are effectively polished off; additionally careful shaping and positioning of the erosion electrodes allows a certain degree of shaping of the polished surface. As a result very thin and uniform surface flex joints are expected. After the electropolishing the shape and the thickness uniformity of the flexures will be checked by X–ray microdensitometry, using as a source an ytterbium wire; for targets few tens of microns thick, this technique allows an accuracy of few parts in 10^3.

Our choice for the material is the beryllium–copper alloy: the Cu–Be has a good thermal stability [8], being the coefficient of thermal expansion $17 \cdot 10^{-6} K^{-1}$, it's not magnetic, its intrinsic loss angle is about 10^{-4} and its yield strength ranges from 700 MPa to 1300 MPa when the material is precipitation hardened (baked at $315\ ^{\circ}C$ for two hours). Fig.10 shows the mechanical drawings of the horizontal accelerometer prototype that we are building; the mechanical design is based on the folded pendulum model proposed in the previous paragraph. The related estimated parameters are the following:

L	81 mm
l_p	71.5 mm
m_{a1}	0.14 Kg
m_{a2}	0.21 Kg
m_{p1}	1.29 Kg
m_{p2}	1.21 Kg
ν_0	254 mHz
M_e	2.69 Kg
A	–0.018
n	8
I	$4 \cdot 10^{-19}$ m^4
κ_{grav}	0.030 N $\cdot$ m^2
κ_{flex}	0.006 N $\cdot$ m^2
dilution factor	5

folded pendulum accelerometer

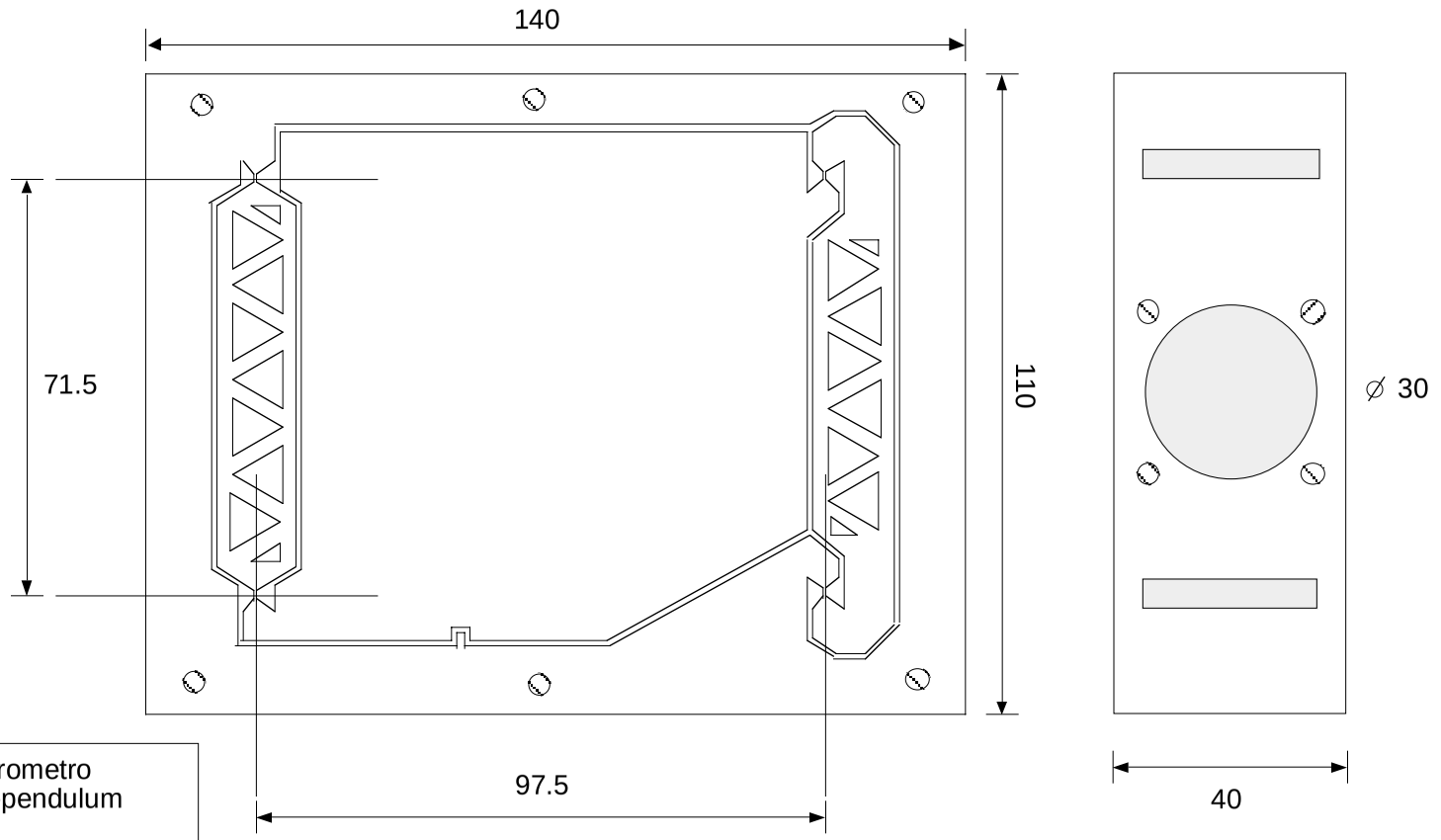

accelerometro
folded-pendulum

materiale: Cu-Be
lavorazione: wire EDM
∅ 100 µm e 50 µm

Fig.10 Mechanical drawing of the FP based accelerometer prototype

Part.#1
braccetto
simple pendulum

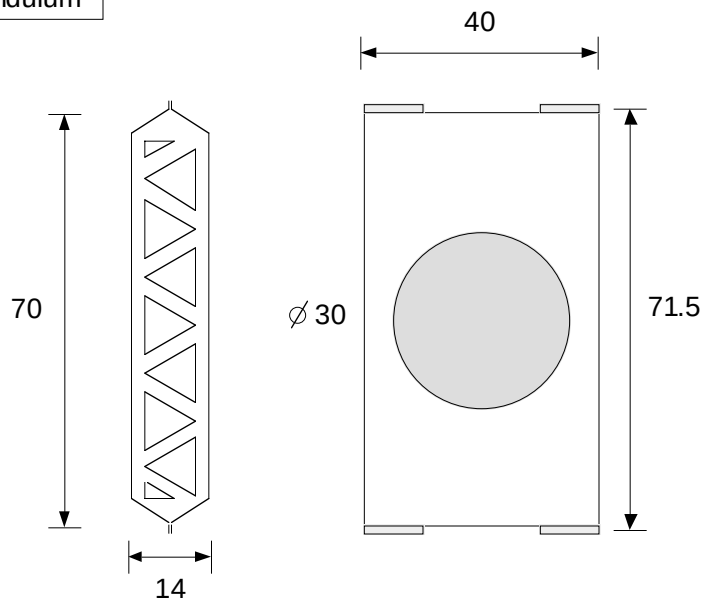

Part.#2
braccetto
inverted pendulum

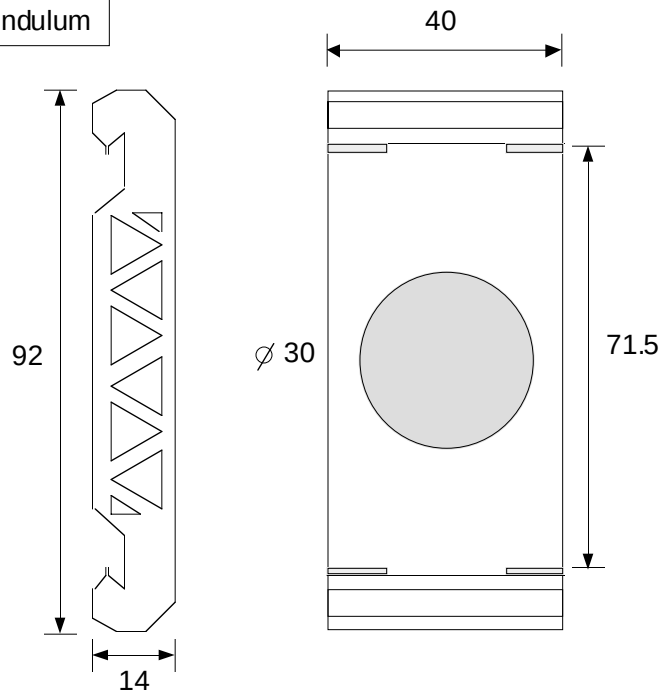

Part.#3
equipaggio
mobile

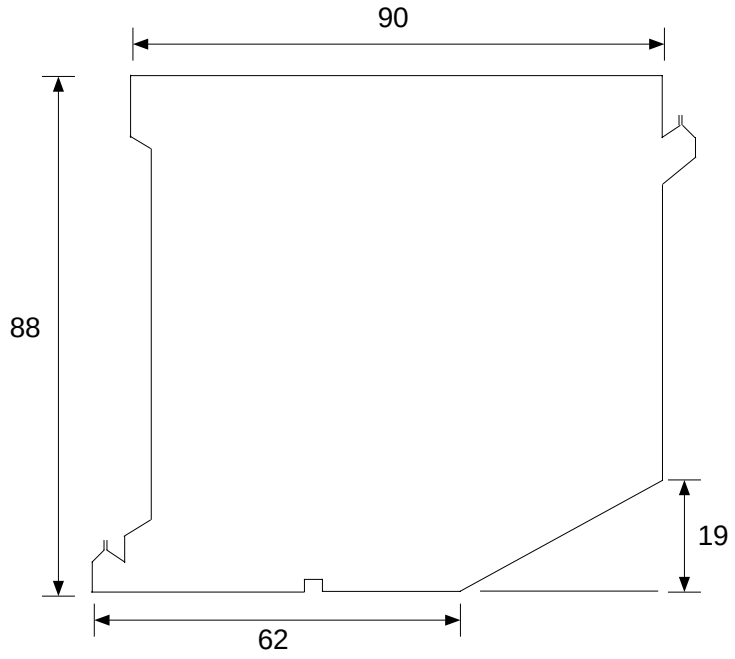

Part.#4
flex joints
lavorazione: EDM e
electropolishing

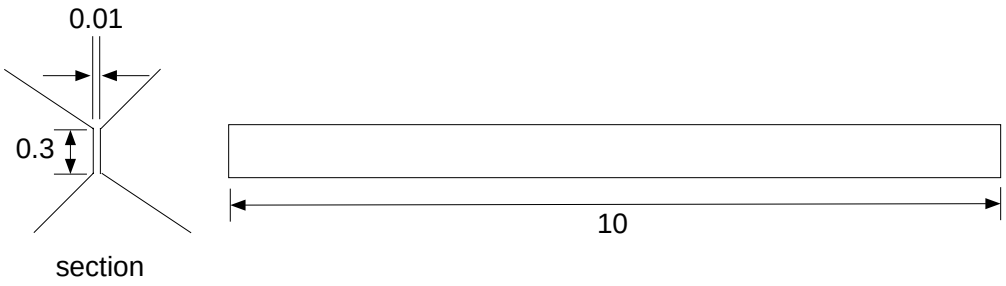

As shown in the drawings the supporting arms are windowed to reduce their momentum of inertia, but preserving the rigidity and yielding relatively high internal resonant frequencies. The arms are also windowed in the longitudinal direction to allow to access to the pendulum bob for the position sensor and the feedback actuator. The sensor and the actuator will be mounted on two caps to be

screwed on the sides of the folded pendulum body. In principle the FP resonant frequency can be design predetermined by distributing the load on the two arms; in practice the frequency can be easily tuned by adding a small tuning mass to the pendulum itself.
In this prototype we will use 8 flex joints 10–μm thick and 10–mm wide, being limited by the machining precision; the load on each of them is only 7 N for a resulting stress of 70 MPa which is small if compared with the yield strength of the beryllium–copper. Each joint is made of two tandem half joints each 10–mm wide separated by a 20–mm gap. Perfect alignment of the two half joints is intrinsic in the wire EDM machining from a monolithic block. The large effective width (40 mm) obtained by the use of tandem half joints maximises the test mass transversal rigidity, thus minimising the acceleration sensitivity to orthogonal movements. The shortness of the joints makes the accelerometer more insensitive to torsional movements. In our design the resulting dilution factor is only 6 being the flexures overdimensioned with respect to the mechanics. The overdimensioning can be later reduced by cutting off some of the 10–mm joint length. For an idealized folded–pendulum accelerometer the sensitivity with respect to the thermal noise is:

$$\tilde{x}_{th.noise} = \frac{1}{M_e l_p}\sqrt{\frac{4K_B T \kappa_{flex}}{Q_0 \omega^5}} \qquad (3.1.1)$$

where Q_0 is the intrinsic Q factor of the material. A numeric evaluation of (3.1.1) yields:

$$\tilde{x}_{th.noise} = 1.5\cdot 10^{-14}\ f^{-5/2} \qquad (3.1.2)$$

for Q_0=1000, that is $\tilde{x}_{th.noise} \approx 4\cdot 10^{-12}\ m/\sqrt{Hz}$ at 100 mHz. This results could represent an improvement of a factor a hundred with respect to the state of art, that is a VIRGO–like accelerometer.

3.2 The position sensor and the actuator

The accelerometer will be equipped with a position sensor and an actuator for feedback closed–loop operation. To match the expected thermal noise the required position sensor sensitivity is $10^{-12}\,m/\sqrt{Hz}$; several devices show performances satisfying this limit. Possible choices are an LVDT [2], an interferometer [9], a point–contact tunneling sensor and a capacitor [10]. This accelerometer has to be used to control the elements of a seismic attenuator; it has to be rugged and assure stable performances in long term operation.
The sensing element has to be rugged and as simple as possible. For instance, a microwave device

like a sapphire–loaded cavity [11] shows extremely low noise, $10^{-15}\mathrm{m}/\sqrt{\mathrm{Hz}}$, but requires cryogenic operation and the readout circuitry is very complex. Consequently it is not suitable to be used in our control system. Tunneling sensors, being developed at University of Pisa [12, 13], show the same level of sensitivity while the signal is simply extracted by an AC coupled Wheatstone bridge. In this sensor the displacement is measured by measuring the change of the resistance of a point–like tunneling junction (Fig.11) formed between a tungsten whisker, having a radius of curvature of 0.1 μm, and a nickel plate; this latter is covered by an insulating nickel oxide film, about 0.1 nm thick, generating a potential barrier of about 1 eV through which the whisker electrons can tunnel when the junction is biased.

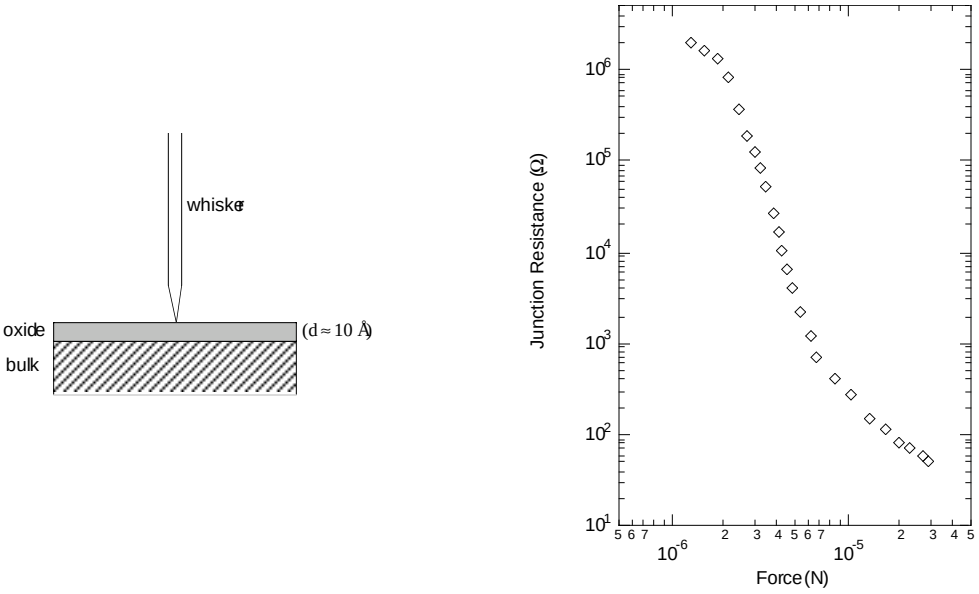

Fig.11 Schematic of tunneling sensor and characteristic response of the device

The contact resistance is strongly dependent on the force applied between the two elements of the junction, due to a combination of two effects: the increase of the contact area and the deformation of the insulating layer. The typical dynamic range is 10^7 with measuring ranges from few nanometers to few microns, depending on the elastic spring stiffness of the whisker mount. A first prototype of a vertical accelerometer using the whisker as sensing element has been built and tested. The defect of this device is its limited ruggedness. The sensor is in contact with the proof mass of the accelerometer and any failure of the feedback system could cause damage of the whisker tip. For this reason at present this option is kept aside for future super–high resolution accelerometrs based on non metallic (quartz) flex joints. The optical readout is a valid option but

an interferometric device has to be implemented on the accelerometer, with lenses, a beam splitter, mirrors and a light source (a laser or a LED). It is capable of sensitivities of the order of $10^{-15}\,\mathrm{m}/\sqrt{\mathrm{Hz}}$ but with a half a fringe dynamic range that is 0.2–0.3 μm for a near–infrared laser source. An even better solution is to use one mirror of the interferometer to track the displacement of the accelerometer mass mirror; the tracking mirror is mounted on an actuator (PZT) and is driven by the filtered signal from the photodetector [14]. This closed–loop tracking interferometer showed a dynamic range of few microns (limited by the actuator) and a shot noise limited sensitivity of $10^{-13}\,\mathrm{m}/\sqrt{\mathrm{Hz}}$. A schematic of this kind of displacement sensors is shown in Fig.12:

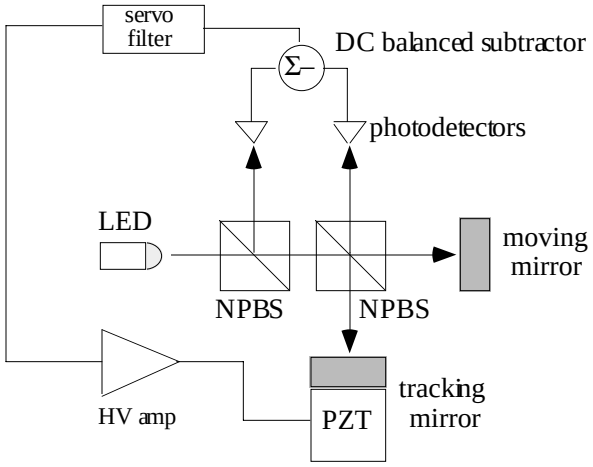

Fig.12 Schematic drawing of a tracking mirror interferometer displacement sensor

The sensor is not very compact (8x8 cm) and powered by a collimated high–efficiency LED; there are not lenses, but only two non–polarizing beam splitters; the DC balanced detection limits the noise due to power fluctuations of the light source. The main readout option we want to investigate is the capacitive one which, coupled with a capacitive actuation, seems to be ideal for our mechanics. A capacitive sensor is simple and rugged and provides a dynamic range between 10^6 and 10^7 so that with a measuring range of few microns is possible with the required sensitivity. For the readout electronics the options are the usual AC coupled capacitive bridge [10] and a LC resonant tank circuit in which the tuning capacitor is the motion sensor itself. At present we are testing an LC FET oscillator operating at 20 MHz with an electrical Q factor of about 30; the tuning capacitor is realized with two $10-\mathrm{cm}^2$ copper plates 0.15–mm spaced; the oscillator output frequency is compared with a stable reference quartz and the beat signal is fed into a monolithic IC frequency–to–voltage converter (LM–2917). This electronic design is very rugged and provides

high resolution: the first prototype, realized with commercial low profile components, showed a dynamic range of about 20 μm with a measured noise of $5 \cdot 10^{-11} \mathrm{m} / \sqrt{\mathrm{Hz}}$ at 1 Hz. The second readout method considered is the resonant phase shift technique [15]: in this case the capacitor is arranged to be the tuning element in a series resonant LC tank circuit driven by a transistor emitter follower. Signal information is extracted by measuring the phase shift in the transistor collector current resulting from any change in the capacitor value. This alternative scheme also provides high resolution and allows to eliminate the frequency–to–voltage converter. The only two options for the actuation are the voice–coil and a capacitor. Although the voice–coil actuator has been demonstrated to be very reliable, we are oriented towards the capacitor, because if the system is not properly designed the magnetic field from the permanent magnet of the voice–coil could damp the accelerometer by eddy–currents. A capacitive actuator seems to be less intrusive, although it is in principle non linear and it has to be linearized by applying a high voltage bias. Eventual losses from surface oxides will be reduced by depositing on the capacitor plates a thin film of gold.

4. Conclusions

We proposed a new high sensitive low frequency horizontal accelerometer to realize a second level of active control in an actively pre–damped seismic isolator. Our effort has been focussed on the mechanics of the device in order to reduce dissipative effects which limit the performances of the available accelerometers at frequencies between 0.01 and 1 Hz. The mechanical design of a prototype, based on the folded pendulum geometry, has been proposed among with an estimation of the potential performances; this mechanics, coupled with an appropriate position sensor, could assure a sensitivity of about $10^{-12} \mathrm{m} / \sqrt{\mathrm{Hz}}$ down to about 150 mHz. Below this frequency thermal noise will affect the device response, even if at 50 mHz the sensitivity could be still $3 \cdot 10^{-11} \mathrm{m} / \sqrt{\mathrm{Hz}}$. The machining of the mechanics from a single piece of material should be a big benefit also for the performances of vertical accelerometers and specially for low frequency tiltmeters for which realization all the gravity wave people are putting a great effort.

References

1 – G. Losurdo *et al.*, Rev. Sci. Instrum. **70**, 2507 (1999).

2 – S. Braccini *et al.*, Rev. Sci. Instrum. **66**, 2672 (1995).

3 – P. R. Saulson, Phys. Rev. D **42**, 2437 (1990).

4 – ????, PhD Thesis, University of Western Australia, in preparation.

5 – D. G. Blair, L. Ju, M. Notcutt, Rev. Sci. Instrum. **64**, 1899 (1993).

6 – T. J. Quinn, C. C. Speake, L. M. Brown, Philos. Mag A **65**, 261 (1992).

7 – G. Cagnoli *et al.*, Phys. Lett. A **213**, 245 (1996).

8 – *Goodfellow Catalogue*, Goodfellow Metals Ltd., England.

9 – D. Rugar, H. J. Mamin, P. Guethner, Appl. Phys. Lett. **55**, 2588 (1989).

10 – P. S. Linsay, D. H. Shoemaker, Rev. Sci. Instrum. **53**, 1014 (1982).

11 – L. Ju, D. G. Blair, H. Peng, F. van Kann, Meas. Sci. Technol. **3**, 463 (1992).

12 – A. Bertolini, *Tesi di Laurea*, Dipartimento di Fisica, Università degli Studi di Pisa (1996), unpublished.

13 – A. Bertolini *et al., JILA Meeting on Seismic Attenuation 1998*, (1998) unpublished.

14 – M. Barton, M. Gray, LIGO internal report, (1998).

15 – G. L. Miller, E. R. Wagner, T. Sleator, Rev. Sci. Instrum. **61**, 1267 (1990).